Gut 64.12 (2015): 1921-1935

DOI: 10.1136/gutjnl-2014-.308935

Microenvironmental hCAP-18/LL-37 promotes pancreatic ductal adenocarcinoma by activating its cancer stem cell compartment

Bruno Sainz, Jr.[1,6], Sonia Alcala[1,6], Elena Garcia[2,8], Yolanda Sanchez-Ripoll[1], Maria M. Azevedo[1], Michele Cioffi[1], Marianthi Tatari[1], Irene Miranda-Lorenzo[1], Manuel Hidalgo[3], Gonzalo Gomez-Lopez[4], Marta Cañamero[5], Mert Erkan[7,11], Jörg Kleeff[7], Susana García-Silva[1], Patricia Sancho[1], Patrick C. Hermann[1,9], and Christopher Heeschen[1,10]

[1]Stem Cells & Cancer Group, Molecular Pathology Programme, [2]Molecular Diagnostics Unit & [3]Gastrointestinal Cancer Clinical Research Unit, Clinical Research Programme, [4]Bioinformatics Unit, and [5]Histopathology Unit, Spanish National Cancer Research Centre (CNIO), Madrid, Spain; [6]Department of Preventive Medicine, Public Health and Microbiology, Universidad Autónoma de Madrid, Madrid, Spain; [7]Department of Surgery, Klinikum rechts der Isar, Technical University, Munich, Germany; [8]Pathology Department, Hospital Universitario Fundacion Alcorcon, Spain; [9]Deptartment of Internal Medicine I, Ulm University, Germany; [10]Centre for Cancer, Stem Cells & Ageing, Barts Cancer Institute, Queen Mary University of London, London, UK.

[11]Current address: Koc University School of Medicine, Istanbul, Turkey

[*]Correspondence: Dr. Bruno Sainz, Jr., PhD, Department of Preventive Medicine, Public Health and Microbiology, Universidad Autónoma de Madrid, E-28029 Madrid, Spain. E-mail: bruno.sainz@uam.es; Dr. Christopher Heeschen, MD, PhD, Centre for Cancer, Stem Cells & Ageing, Barts Cancer Institute, Queen Mary University of London, London, UK. E-mail: c.heeschen@qmul.ac.uk

Word count: Abstract: 250 words / Text: 4,171 words

Running title: *LL-37/hCAP18 and pancreatic cancer stem cells*

Keywords: hCAP-18/LL-37, pancreatic cancer, cancer stem cells, tumour-associated macrophages, tumour microenvironment

Abbreviations:

CSC: cancer stem cells
PDAC: pancreatic adenocarcinomas
hCAP-18/LL-37: human cationic antimicrobial peptide 18/LL-37
LL-37: leucine leucine 37
rLL-37: recombinant leucine leucine 37
TAM: tumour-associated macrophage
TGF-β1: tumor growth factor-β1
FPR2: formyl peptide receptor 2
P2X7R: P2X purinoceptor 7 receptor (P2X7R)
CAMP: cathelicidin antimicrobial peptide
CRAMP: cathelicidin-related antimicrobial peptide
PSC: pancreatic stellate cell
PDX: patient-derived xenografts
KPC: K-Ras$^{+/LSL-G12D}$;Trp53$^{LSL-R172H}$;PDX1-Cre
RT-qPCR: Real-time quantitative polymerase chain reaction
RSAD2: radical S-adenosyl methionine domain containing 2
CMPK2: cytidine monophosphate (UMP-CMP) kinase 2
KRT19: kertain 19
SIGLEC1: sialic acid binding Ig-like lectin 1
ORM1: orosomucoid 1
TMA: tissue microarray
YM1: chitinase 3-like 3
F4/80: macrophage (M phi)-specific monoclonal antibody
CXCR4: C-X-C chemokine receptor type 4
EMT: epithelial to mesenchymal transition
GM-CSF: granulocyte-macrophage colony-stimulating factor
CM: conditioned medium
OSM: oncostatin M
VEGF: vascular endothelial growth factor
VDR: vitamin D receptor
Alk4: Activin-like 4
CTCs: circulating tumour cells
EPCAM: epithelial cell adhesion molecule
PanIN: pancreatic intraepithelial neoplasia
OAS: (2'-5') oligo A synthetase
MX1: nterferon-induced GTP-binding protein
ISG15: interferon stimulated gene 15
GEM: gemcitabine

ABSTRACT

Objectives: The tumour stroma/microenvironment not only provides structural support for tumour development, but more importantly it provides cues to cancer stem cells (CSC) that regulate their self-renewal and metastatic potential. This is certainly true for pancreatic adenocarcinomas (PDAC), where tumour-associated fibroblasts, pancreatic stellate cells and immune cells create an abundant paracrine niche for CSCs via microenvironment-secreted factors. Thus understanding the role that tumour stroma cells play in PDAC development and CSCs biology is of utmost importance.

Design: Microarray analyses, tumour microarray immunohistochemical assays, *in vitro* co-culture experiments, recombinant protein treatment approaches and *in vivo* intervention studies were performed to understand the role that the immuno-modulatory cationic antimicrobial peptide 18/LL-37 (hCAP-18/LL-37) plays in PDAC biology.

Results: We found that hCAP-18/LL-37 was strongly expressed in the stroma of advanced primary and secondary PDAC tumours and is secreted by immune cells of the stroma (eg, tumour-associated macrophages) in response to TGF-β1 and particularly CSC-secreted Nodal/ActivinA. Treatment of pancreatic CSC with recombinant LL-37 increased pluripotency-associated gene expression, self-renewal, invasion, and tumourigenicity via formyl peptide receptor 2 (FPR2)- and P2X purinoceptor 7 receptor (P2X7R)-dependent mechanisms, which could be reversed by inhibiting these receptors. Importantly, in a genetically engineered mouse model of K-Ras-driven pancreatic tumourigenesis, we also showed that tumour formation was inhibited by either reconstituting these mice with bone marrow from CRAMP (i.e murine homolog of hCAP-18/LL-37) knockout mice or by pharmacologically inhibiting FPR2 and P2X7R.

Conclusion: Thus, hCAP-18/LL-37 represents a previously unrecognized PDAC micro-environment factor that plays a critical role in pancreatic CSC-mediated tumourigenesis.

SIGNIFICANCE OF THE STUDY

What is already known on this subject?

- Pancreatic ductal adenocarcinoma (PDAC) is the most lethal cancer with limited therapeutic options.
- Pancreatic cancer stem cells (CSCs) are exclusively tumourigenic and highly resistant to chemotherapy.
- Tumour-associated macrophages are important for the progression and metastatic spread of many solid tumours.

What are the new findings?

- The immuno-modulatory cationic antimicrobial peptide 18/leucine leucine-37 (hCAP-18/LL-37) is over expressed in the stroma of PDAC and acts on CSCs to potentiate their inherent biological properties.
- Tumour-associated macrophages secrete hCAP-18/LL-37 in direct response to CSC-secreted NODAL/ACTIVINA/TGF-β1.
- Small molecule targeting of the LL-37 receptors formyl peptide receptor 2 (FPR2) and P2X purinoceptor 7 receptor (P2X7R), present on pancreatic CSCs, negatively impacts tumour growth and circulating tumour cell numbers.

How might it impact on clinical practice in the foreseeable future?

- The discovery of the crucial role of hCAP-18/LL-37 in cancer stem cell biology represents an important advancement in our understanding of the PDAC tumour microenvironment.
- Targeting pancreatic CSCs using inhibitors of the LL-37 receptors FPR2 and P2X7R may represent a specific therapeutic approach to block the tumour promoting cross-talk that exists within the tumour microenvironment.

INTRODUCTION

Pancreatic ductal adenocarcinoma (PDAC) is one of the most aggressive cancers largely due to its high resistance to current treatment strategies[1]. This can at least, in part, be attributed to a subpopulation of cells known as pancreatic cancer stem cells (CSCs)[2, 3, 4], which are defined by their cell-intrinsic and unlimited self-renewal, exclusive long-term tumourigenicity, capacity to recapitulate the entire cancer cell heterogeneity, and metastatic potential[5, 6, 7]. In addition, PDAC is characterized by extensive desmoplasia[8], which is made up of heterogeneous cell populations, including pancreatic stellate cells (PSCs)[9, 10] and immune cells[8, 11, 12, 13, 14, 15]. This dynamic cellular microenvironment may directly or indirectly promote CSCs features[6, 10, 16, 17], but few comprehensive studies have been performed in PDAC to date. Thus, we set out to identify stroma-specific paracrine drivers that potentiate pancreatic CSC features.

Here we show that the human cationic anti-microbial protein 18 (hCAP-18, CAMP), the only known human cathelicidin alarmin[18, 19, 20], is strongly and exclusively expressed by macrophages present within the PDAC stroma. Cleavage of hCAP-18 at the COOH-terminal end gives rise to the biologically active 37 amino acid hCAP-18 peptide called leucine leucine-37 (LL-37)[19, 20]. Intriguingly, secreted LL-37, via the G protein–coupled receptor, formyl peptide receptor 2 (FPR2)[21, 22, 23] and P2X(7) purinergic receptor[22], significantly potentiated pancreatic CSC features, such as self-renewal, invasion and tumourigenesis. While the factors that mediate LL-37 expression can vary based on the biological context, we also show for the first time that CSC-secreted TGF-β family members Nodal and ActivinA induce hCAP-18/LL-37 expression in macrophages. Pharmacological or genetic inhibition of paracrine activation of pancreatic CSCs by LL-37 markedly reduced their tumourigenicity and metastasis *in vivo*. Thus, our findings not only identify a previously unrecognized tumour microenvironment factor that potentiates pancreatic CSC features, but also highlight the potential therapeutic impact that targeting this peptide may have on PDAC progression and spread.

METHODS

Primary human pancreatic cancer cells and macrophages. The use of human material was approved by the local ethics committee of each respective hospital or university, and written informed consent was obtained from all patients. Tumours were expanded in mice as xenografts (PDX), processed and subsequently cultured *in vitro* as previously detailed[7]. Human blood was obtained from healthy donors with informed consent. Monocyte-derived human macrophage cultures were established and polarized to an M1 phenotype with GM-CSF as previously described[24, 25, 26].

Tissue microarrays (TMAs) Four human TMAs containing quadruplicate 1mm cores from a total of 42 tumours were constructed. The use of human tissue samples for the construction of the TMAs was approved by the Ethics Committee of the Hospital de Madrid Norte Sanchinarro. All immunohistochemically-stained sections were assessed and scored by in-house pathologists.

In vivo assays. The K-Ras$^{+/LSL\text{-}G12D}$;Trp53$^{LSL\text{-}R172H}$;PDX1-Cre mouse model (KPC) of advanced pancreatic cancer has been described previously[27]. B6.129X1-Camp^{tm1Rlg}/J mice (CRAMP$^{-/-}$) were purchased from Jackson Laboratories (Bar Harbor, Maine) and have been previously described[28]. Mice were housed according to institutional guidelines and all experiments were approved by the Animal Experimental Ethics Committee of the Instituto de Salud Carlos III (Madrid, Spain).

Statistical analyses. Results for continuous variables are presented as means ± standard error of the mean (SEM) unless stated otherwise. Treatment groups were compared with the independent samples t test. Pair-wise multiple comparisons were performed with the one-way ANOVA (two-sided) with Bonferroni adjustment. P values <0.05 were considered statistically significant. All analyses were performed using SPSS 22.0 (SPSS Inc., Chicago, IL).

More Materials and Methods can be found as online supplementary information.

RESULTS

Macrophages promote PDAC tumourigenesis and produce hCAP-18/LL-37. To appreciate the contributory role of tumour stroma cells in PDAC development, we injected into nude mice 5×10^5 primary sphere-derived CSC-enriched PDAC cells alone or with equal numbers of immortalized PSCs, primary PSCs or primary human monocyte-derived unpolarized macrophages. No marked differences in early tumour growth were observed between primary PDAC cells injected alone or with PSCs. In contrast, tumour take and growth was significantly accelerated when PDAC cells were co-injected with macrophages (**Fig. 1A**). Interestingly, at 1.5 weeks human macrophages were no longer detected in these tumours as determined by a lack of CD68, CD16 and CD163 staining (**data not shown**), suggesting that the transient presence of human macrophages was sufficient to jumpstart tumour take and promote PDAC cell growth *in vivo*.

To begin to understand how macrophages might promote PDAC tumour growth, we co-cultured human monocyte-derived unpolarized macrophages with and without primary PDAC cells in trans-wells (to separate the two cell types) and performed microarray analyses (**Table S1**). Of the top 25-up-regulated genes in macrophages (FDR<10^{-4}, $|\log FC|>2$), 19 genes belonged to the family of interferon-stimulated genes (**Fig. 1B**), while the 6 remaining genes (RSAD2, CMPK2, KRT19, CAMP, SIGLEC1, and ORM1) encoded for proteins with diverse functions. We identified hCAP-18/LL-37 (ie, CAMP) as a gene of interest as it both encodes for a secreted factor and has been shown to be expressed in other solid tumours, including breast[29, 30], lung[31, 32, 33] and ovarian cancers[18, 23, 34], albeit in the epithelial compartment. RT-qPCR analysis (**Fig. 1C**) and immunofluorescence confocal microscopy (**Fig. 1D**) showed up-regulation of hCAP-18/LL-37 in monocyte-derived unpolarized macrophages only when co-cultured with primary PDAC cells, validating our microarray results. Moreover, while PDAC cells co-cultured with macrophages did not express hCAP18/LL-37 (data not shown), we observed up-regulation of pluripotency-associated genes, which was blocked by the addition of LL-37 blocking antibodies or inhibitors, suggesting an LL-37-mediated cross talk between macrophages and CSCs (**Fig. 1E and S1**).

Primary PDAC tumours express hCAP-18/LL-37. Next, we assessed the expression of hCAP-18/LL-37 by RT-qPCR and immunohistochemical (IHC) analysis in primary PDAC samples. Compared to normal pancreas, over expression of hCAP-18/LL-37 mRNA and protein was observed in all PDAC samples (**Fig. 2A** and **S2A**). Interestingly, only the stroma stained positive for hCAP18/LL-37 while cancer cells were negative (**Fig. 2A** and **S2A-C**), which is in contrast to what has been reported for other carcinomas[18, 29, 31, 35].

Data were extended using tissue microarrays. The majority (~74%) of 'normal' adjacent non-tumour tissue was negative for hCAP-18/LL-37; however, 81% of PDAC samples stained positive for LL-37 with varying degrees of intensity observed between tissues (**Fig. 2B-C** and **S2-S3**). Staining of serial sections for LL-37, CD16, CD163, CD68 and αSMA demonstrated that tumour infiltrating immune cells (ie, macrophages) were the predominant cell type producing hCAP-18/LL-37 (**Fig. 2D** and **S2D-E**); however, other stromal cells (eg, $CD16^{+}$ neutrophils) also expressed LL-37.

To allow for a more systematic analysis of pancreatic cancer progression from low to high grade PanINs, PDAC lesions, and subsequent metastatic spread we next studied the $K\text{-}Ras^{+/LSL\text{-}G12D}$;$Trp53^{+/LSLR172H}$;PDX-1-Cre (hereafter referred to as KPC)[27] mouse model of PDAC. CRAMP (ie, murine homolog of hCAP-18/LL-37) expression in KPC mice was similarly restricted to the tumour stroma, absent in normal tissue, and most prominently expressed in primary PDAC lesions and in all metastatic lesions of secondary organs, such as the liver (**Fig. 2E** and **S4A**). Staining for the macrophage markers YM1 or F4/80 also revealed a strong correlation between macrophages and CRAMP staining (**Fig. 2E, S4B-C**).

CRAMP promotes tumourigenicity of murine PDAC cells in vivo. To test whether CRAMP expression is necessary for tumour formation *in vivo*, we eliminated CRAMP from the hematopoietic system of irradiated 5-6 week old KPC mice by syngeneic transplantation of either wild-type or CRAMP knockout ($CRAMP^{-/-}$) bone marrow. While all mice, regardless of the donor bone marrow received, showed macrophage infiltration in the pancreas (**Fig. S5A**), mice transplanted with bone marrow from $CRAMP^{-/-}$ mice did not show any CRAMP expression, which does not only suggest excellent

transplantation efficiency but also demonstrates that immune cells and not other stromal cells are the primary source of CRAMP in PDAC tumours (**Fig. 3A**). At the tumour level, PDAC tumour tissue and severely altered tissue [ie, acinar-to-ductal metaplasia (ADM) and inflammation (**Fig. S5B**)] were significantly reduced in mice transplanted with CRAMP$^{-/-}$ bone marrow compared to controls at 17 weeks post transplantation (**Fig. 3B** and **S5C**).

To rigorously test the effects of CRAMP on the *in vivo* CSC compartment, which are exclusively capable of tumour initiation and progression[36], we next performed limiting dilution cell transplantation assays. Primary syngeneic murine PDAC sphere-derived cells expressing a luciferase reporter were transplanted into recipient wild-type and CRAMP$^{-/-}$ mice and tumour formation was determined 5 weeks post injection (**Fig. 3C**, **left**). While tumours efficiently formed in wild-type mice at dilutions of 10^4 (4/8) and 10^5 (8/8) cells, only one tumour was detected in CRAMP$^{-/-}$ mice injected with 10^5 (1/8) cells, indicating that the capacity for CSC-initiated tumourigenesis was significantly reduced in CRAMP$^{-/-}$ mice (**Fig. 3C**, **right**). In addition, we found a clear reduction in the percentage of CD133+ cells in the tumour formed in the CRAMP$^{-/-}$ mouse (**Fig. 3D**). To further dissect these phenotypes at the macrophage level, we injected 5×10^5 primary sphere-derived CSC-enriched murine PDAC cells alone or with equal numbers of monocyte-derived unpolarized macrophages isolated from wild-type or CRAMP$^{-/-}$ mice. After 4 weeks, tumour take and growth was significantly accelerated when murine PDAC cells were co-injected with wild-type macrophages [similar to what was observed when human macrophages were co-injected with human PDAC cells (**Fig. 1A**)], but not with CRAMP$^{-/-}$ macrophages (**Fig. 3E**). In line with these observations, murine PDAC sphere formation was consistently enhanced in the presence of wild-type macrophages versus CRAMP$^{-/-}$ macrophages (**Fig. S5D**), suggesting that CRAMP enhances/promotes PDAC tumour take and progression by potentiating CSC *in vivo* self-renewal and tumourigenesis.

hCAP18/LL-37 has inherent pro-CSC properties. Stimulated by these proof-of-concept studies, we next aimed to further dissect the mechanisms of action for LL-37 on human pancreatic cancer (stem) cells. Using the established CSC cell surface marker CD133[2] and a novel biomarker for CSC,

autofluorescence[5], we found that treatment of primary xenograft-derived PDAC cultures with recombinant LL-37 peptide (rLL-37) resulted in a consistent ~2-fold enrichment in the CD133+ (**Fig. 4A** and **S6A**) and autofluorescent populations (**Fig. 4B** and **S6A**), suggesting that LL-37 increases the CSC pool. Indeed, colony-forming (**Fig. 4C**), and sphere-forming efficiency (**Fig. 4D**) were both significantly enhanced by rLL-37; the latter even more pronounced during serial passaging, which further enriches for CSCs (**Fig. 4D**). Treatment also resulted in over expression of *KLF4, SOX2, OCT3/4,* and *NANOG* in rLL-37-treated spheres (**Fig. 4E** and **S6B-C)**. Of note, recombinant CRAMP functioned similarly to rLL-37 in CSCs derived from KPC mouse pancreatic tumours (**Fig. S7**). Lastly and in line with a pro-CSC effect, rLL-37 also increased the inherent chemoresistant potential of CSCs, as measured by increased CD133+ cells following treatment with Gemcitabine or Abraxane (**Fig. 4F** and **S8**).

Importantly, the most defining feature of CSCs lies in their ability to form tumours *in vivo*. Sphere-derived PDAC cells pre-treated with rLL-37 revealed consistently enhanced tumourigenicity, a higher CSC frequency, and increased early tumour take as compared to scrambled peptide-treated cells. Notably, this effect was particularly evident when low cell numbers (~10 cells) were injected (**Fig. 5A-B**). In line with our hypothesis that the effects of LL-37 are preferentially affecting CSCs, when we injected adherent cells, which contain few CSCs[6], the differences in tumourigenicity between non-treated and rLL-37-treated cells were not as striking (sphere-derived cells: 10.2-fold [CI 10.1-10.4] increase in CSC frequency; adherent cells: 1.4-fold [CI 1.3-1.5] increase in CSC frequency) (**Fig. S9**). Lastly and to more rigorously test the hypothesis that LL-37 more specifically promotes CSCs, we assessed the sphere forming capacity and cell cycle profile of CD133+ CSC and their CD133– counterparts in the absence or presence of rLL-37. Indeed, our data confirm that LL-37 preferentially targets and potentiates CSC self-renewal and proliferation **(Fig. 5C-D)**.

LL-37 promotes CSC invasiveness. We found the highest expression of LL-37 and CRAMP in primary PDAC tumours and metastatic lesions of human and mouse origins (**Fig. 2**), respectively, suggesting that LL-37 is likely important late during PDAC progression and may be involved in EMT. Supporting this hypothesis, rLL-37 treatment increased the CXCR4+ subpopulation (**Fig. 6A**) present in

CSCs, a subpopulation of CSCs that drives metastasis[2]. Analysis of EMT-related genes following rLL-37 treatment revealed down-regulation of E-cadherin and up-regulation of Vimentin and Snail (**Fig. 6B-C**), and rLL-37 treatment also increased migration (**Fig. 6D**) and invasion of CSCs (**Fig. 6E**). Of particular interest, chemoattraction of invading rLL-37-treated sphere-derived PDAC cells by the CXCR4 ligand SDF-1 was evident even at very low concentrations (eg, 1ng/mL), which had no impact on control cells. To validate this *in vivo*, we intraspleenically injected rLL-37 pre-treated CSCs stably expressing a luciferase reporter and observed increased dissemination (ie, micro-metastases) of cells pre-treated with rLL-37 to the liver (**Fig. 6F-G** and **S10**).

Macrophages express hCAP-18/LL-37 in response to CSC-secreted TGF-β1 family members. Macrophages (ie, TAMs), as one of the primary sources of LL-37 *in vivo,* may respond to cues from the tumour (eg, CSC) to drive the expression of LL-37. To further dissect this putative CSC-TAM crosstalk, we modeled the tumour *in vivo* microenvironment by first polarizing monocyte-derived human macrophages towards an 'M1' phenotype with GM-CSF[24] prior to exposing them to CSC-conditioned media (CM). Intriguingly, 'M1' macrophages exposed to CSC CM up-regulated LL-37 (**Fig. 7A-B**) and underwent a morphological change from a classic circular morphology to a more elongated shape (**Fig. 7C**). This change was accompanied by induction of alternatively-activated/'M2' genes, such as oncostatin M (OSM) and VEGF (**Fig. 7D**) as well as fluctuations in the expression of the cell surface M2 macrophage markers CD163, CD204 and CD206[37, 38, 39] (**Fig. S11**).

TGF-β can polarize 'M1' macrophages to an 'M2'/alternatively activated phenotype[40] and cancer cells, including PDAC cells do secrete large amounts of TGF-β (**Fig. S12A**)[41]. As many advanced PDAC tumours harbor inactivating mutations in the TGF-β signaling pathway rendering them unresponsive[42], we reasoned that TGF-β secreted by PDAC cells may instead primarily act on macrophages inducing LL-37 expression. In addition, we recently showed that PDAC CSC over express other member of the TGF-β superfamily, namely Nodal/ActivinA[6], which may also be implicated in the macrophage-CSC-crosstalk. Indeed, pre-treatment of M1-polarized GM-CSF-treated monocyte-derived human macrophages with the TGFβ family members Nodal/ActivinA or TGF-β significantly increased

LL-37 levels (**Fig. 7E-F**) as well as alternatively-activated/'M2' genes, such as OSM and VEGF (**Fig. 7G**) and phospho-p38, NF□B phospho-p50 and the transcription factor vitamin D receptor (VDR) (**Fig. S12B-C**), the latter three of which have been shown to regulate hCAP18/LL-37 expression. Blocking Nodal/ActivinA/TGF-β□ signaling in CSC CM-treated macrophages with SB431542 and SB505124, both of which are inhibitors of the respective receptors *A*ctivin-*lik*e 4 (Alk4) and Alk5, abolished the enhanced expression of LL-37 and additional target genes (**Fig. 7H**).

Targeting LL-37 signaling impairs CSC tumourigenesis. hCAP-18/LL-37 is believed to exert its effects through the receptors FPR2[21, 22] and/or P2X7R[22, 43] (**Fig. 8A**), both of which were detectable at the mRNA level and by flow cytometry in several primary PDAC cultures (**Fig. 8B-C** and **Fig. S13A**). Receptor expression was restricted to a small subpopulation of adherent cells (less than 1%), which increased when cells were cultured as spheres (2-5%) and treated with rLL-37 (4-8%). More importantly, the expression of both receptors was primarily (>60%) restricted to CD133+ cells (**Fig. 8C** and **Fig. S13A**). The latter was particularly evident in a freshly digested PDAC patient tumour (**Fig. S13B**). These data together suggest an enrichment of these receptors in CSCs. Using inhibitors specific for both FPR2 and P2X7R (WR-W4 and KN-62, respectively), LL-37-induced colony formation (**Fig. 8D**), invasion (**Fig. 8E**) and CD133+ cell expansion (**Fig. 8F**) was reduced with each inhibitor alone or in combination, confirming that the effects of LL-37 are indeed mediated through these receptors.

To rigorously test the therapeutic potential of anti-LL-37 therapy *in vivo*, we treated KPC or KPCR (KPC mice that additionally express a pancreas-specific RFP reporter) mice with WR-W4 and KN-62 for either 5 weeks (short-term) or 16 weeks (long-term) (**Fig. 9A**). With as little as 5 weeks of treatment, there was a marked reduction in the number of RFP+ circulating tumour cell of KPCR mice (**Fig. 9B**). In addition, we observed reduced numbers of low-grade PanINs and significantly fewer high-grade PanINs and PDAC lesions (**Fig. 9C**) in treated mice. Of note, no liver metastases were detected in either group at this stage. By extending our treatment to 16 weeks, the number of CTCs (EPCAM+) in treated mice were still reduced (**Fig. 9D**). With respect to the pancreas, while no impact on the incidence of low-grade PanINs was observed, we still quantified significantly fewer high-grade PanINs and PDAC

lesions (**Fig.9E**) in treated mice. In addition, and in line with our CTC analyses, liver metastases were histologically detected in 75% of untreated mice, while only one treated mouse developed liver metastasis (**data not shown**). These results, in their entirety, highlight the promising therapeutic potential of targeting LL-37 signaling in PDAC.

CONCLUSION / DISCUSSION

While the PDAC tumour microenvironment is composed of many different cells, TAMs are likely one of the most dynamic resident cells of the tumour stroma[12, 13, 14, 16, 17, 39, 44, 45]. Not only can they enhance tumour growth when co-injected *in vivo*, but our microarray analyses additionally showed that monocyte-derived human macrophages are transcriptionally re-programmed by PDAC cells. For example, macrophages up-regulated a large number of genes belonging to the family of interferon-stimulated genes (OAS, MX1, ISG15, etc.), which we hypothesize is due to IFN-β produced by PDAC cells[46], similar to what has been shown for other Kras-transformed tumours[47]. Macrophages also down-regulated the expression of chemokines and pro-inflammatory genes, such as CXCL1, CXCL2, IL-1 and IL-6, as well as macrophage M1 markers, such as CD68, thus providing a first indication that PDAC cells alter the differentiation/polarization state of macrophages. Most intriguingly, however, macrophages also up-regulated the expression of hCAP18/LL-37, a peptide previously reported to be either pro- or anti-tumourigenic in other cancer models[18, 29, 48, 49], but had not yet been studied in the context of pancreatic CSC to date and revealed several interesting and novel findings.

The antimicrobial peptide hCAP18/LL-37 was detectable across a large set of PDAC tumours at both the mRNA and protein level, and its expression was most prominent in PDAC and secondary metastatic lesions. hCAP18/LL-37 was originally identified as a host immune anti-microbial defensin molecule and is constitutively secreted by a variety of immune cells (eg, neutrophils and macrophages), but can also be expressed by epithelial cells and fibroblasts[50]. Interestingly, human and murine PDAC epithelial cells were univocally negative for hCAP18/LL-37 or CRAMP, respectively, although previous

studies examining breast, lung, and ovarian cancers had shown that hCAP18/LL-37 is expressed by the tumour epithelium[18, 29]. Instead, in PDAC, expression of hCAP18/LL-37 was clearly restricted to the tumour stroma, revealing a previously unappreciated and important difference between tumour entities with respect to the source of hCAP18/LL-37 expression. We predict that PDAC cells may be deficient in certain signaling factors that are necessary for hCAP18/LL-37 expression, such as vitamin D activated PPARγ signaling[51], NF-κB-mediated CCAAT/enhancer-binding protein α (C/EBP□) activation via MAPK-mediated phosphorylation[52], or other yet unidentified pathways. Within the tumour stroma, we identified macrophages as the primary source of LL-37; however, polymorphonuclear neutrophils can also secrete LL-37[50] and have been shown to be one of the many types of tumour infiltrating cells detected in pancreatic neoplasias[53]. Thus, while we focused on TAMs, we note that other immune infiltrating cells likely also produce LL-37 *in vivo*.

LL-37 has been shown to signal through P2X7R and FPR2[21, 22, 23], both of which were detectable on the surface of PDAC cells, and their expression were primarily restricted to CSCs (ie, CD133+ cells). As CSCs are the driving subpopulation of cells in PDAC with exclusive tumourigenic potential, and since tumour take and growth was significantly increased when PDAC cells were co-injected with macrophages, we thus reasoned that macrophages potentiate tumour growth via an LL-37-mediated pro-CSC mechanism. We confirmed this hypothesis *in vivo* by using CRAMP knockout mice as a source of bone marrow for transplantation experiments in irradiated KPC mice, as a syngeneic model to study CSC-mediated tumour take and growth or as a source of monocyte-derived macrophages for co-injection tumourigenicity studies with murine PDAC CSCs. All three approaches conclusively demonstrated that CRAMP is necessary for CSC-mediated PDAC development and progression *in vivo*. Importantly, these results are in agreement with those published by Li *et al.,* where they show that cathelicidin (ie, CRAMP) expressed from murine myeloid cells promotes cigarette smoke-induced lung tumour growth *in vivo*[32, 33].

To validate the biological relevance of our *in vivo* findings in the human setting, we showed that rLL-37 increased the CSC pool using two independent markers for CSCs (ie, CD133 and

autofluorescence). This apparent activation/stimulation of the CSC compartment was validated at the functional level and during *in vivo* limiting dilution tumourigenicity assays, where we demonstrate that rLL-37 treatment increases sphere-derived CSC-mediated tumour formation and fitness. While sphere-derived cells are enriched in CSCs, tumour growth following injection of low numbers of sphere-derived cells is rarely achieved at single digit numbers. Treatment of cells with rLL-37, however, further expanded the CSCs pool during sphere culture translating into a significantly higher CSC frequency and an apparent increase in viability, such that when injected at low numbers CSCs were able to survive in the recipient host and form tumours. In addition, while it is known that the population of CD133+ CSCs enrich during chemotherapy, we show that rLL-37 treatment further augments this enrichment in the presence of either Gemcitabine or Abraxane, arguing that LL-37 can enhance the inherent chemoresistance of CSCs. These results parallel those of Acharyya S *et al.,* wherein they show that the chemokine S100A8/9, secreted by myeloid cells in the breast cancer microenvironment, also enhances cancer cell chemoresistance[54].

LL-37 treatment also activated an EMT-like profile in CSCs. We observed increased phosphorylation of the kinases ERK1/2, AKT and PKC within 10 minutes of rLL-37 treatment in CSCs, and the EMT transcriptional mediators Vimentin and Snail were additionally up-regulated. At the functional level, rLL-37 treatment increased cell motility and invasion and more importantly increased metastasis *in vivo*. Of particular interest was the observation that rLL-37-treated CSCs were able to invade towards the chemo-attractant SDF-1 at concentrations of only 1ng/mL, while invasion of control cells required 100ng/mL, a concentration that is hardly relevant *in vivo*. Wu *et al.,* reported that rLL-37 enhances the responsiveness of hematopoietic stem progenitor cells to an SDF-1 gradient by CXCR4 cell surface stabilization[55]. In line with these findings, we observed a 3-fold increase in CXCR4 cell membrane expression in rLL-37-treated cells, indicating that LL-37 likely primes CSCs for the SDF-1/CXCR4 axis via a similar CXCR4-dependent mechanism.

Members of the TGF-β superfamily, namely Bone Morphogenic Proteins, TGF-β□, and Nodal/ActivinA, exert multiple and sometimes opposing effects on a variety of cell types. We have

previously shown that TGF-β□ and Nodal/ActivinA are produced by PDAC CSCs and stromal cells[10], while only Nodal/ActivinA directly promote CSC-mediated tumourigenesis[6]. In this study we demonstrate that these CSC-secreted factors also stimulate macrophages in a paracrine fashion. For example, treatment of 'M1'-polarized macrophages with CSC-conditioned media rapidly polarized macrophages towards an alternatively activated phenotype at the morphological, transcriptional and cells surface receptor level. More importantly, we also observed a marked increase in hCAP18/LL-37 mRNA and protein expression following treatment. While Li *et al.*, also showed that ovarian cancer cells can activate *in vitro* cultured macrophages to produce hCAP18/LL-37 via cancer cell secreted versican V1[33], we did not detect expression of versican V1 in our primary PDAC cultures (data not shown). Instead, we identified TGF-β□, Nodal and ActivinA as the factors responsible for CSC-mediated activation of macrophages, and inhibitors of both the TGF-β□ and Nodal/Activin receptors (Alk5 and Alk4, respectively) could reverse the effects *in vitro* and *in vivo* (data not shown). While the transcriptional regulation of hCAP18/LL-37 expression has not been fully elucidated, the CAMP gene is a direct target of the VDR transcription factor[33, 56] and hCAP/LL-37 expression has also been shown to be regulated by NFkB phospho-p50 and phospho-p38[52]. In macrophages treated with CSC-conditioned media or TGF-β□, Nodal and ActivinA, NFkB phospho-p50 and phospho-p38 activation was observed as well as transcriptional upregulation of VDR, implicating these factors as common mediators by which TGF-β superfamily members regulate LL-37 expression and thus promote formation of a pro-CSC niche.

Targeting the tumour microenvironment has gained enormous attention over the past decade, particularly the development of agents that can disrupt the crosstalk between cancer cells and the stroma. Having determined that the majority of cells expressing LL-37 receptors are also CD133+, we tested the efficacy of targeting FPR2 and P2X7R in the clinically relevant KPC PDAC mouse model. We observed that in mice treated with WR-W4 and KN-62, high grade PanIN and PDAC lesions were significantly reduced, and CTCs were essentially eliminated from the blood of treated mice, confirming that LL-37 signaling is indeed important for PDAC tumour progression and dissemination. It is important to note that in

the intervention studies performed in KPC mice we cannot rule out the fact that the treatments used may have also targeted TAMs, which also express FPR2 and P2X7R. Nevertheless, our data provide clear proof of principle for targeting these LL-37 receptors, although more studies will be needed to understand how WR-W4 and KN-62 reduced PDAC progression *in vivo* (ie, at the level of the cancer cell, TAM or both).

Acknowledgements: We are indebted to Sara M. Trabulo and Alexandra Aicher for their technical *in vivo* assistance and to the CNIO Histopathology Core Unit, in particular Raquel Pajares and Maria Lozano.

Contributors: BSJr developed the study concept, obtained funding, acquired, analyzed, and interpreted data and wrote the manuscript; SA assisted in the development of the study concept, acquired, analyzed, and interpreted data. YS-R, MMA, MC, MT, IM-L, GGL and SG-S acquired and analyzed data; MC and EG analyzed and scored histological samples; MH, ME and JK provided extensively characterized PDAC and PSC samples; EG, PS and PH assisted in the development of the study concept, interpreted the data and edited the manuscript; CH developed the study concept, obtained funding, interpreted the data, and wrote the manuscript.

Funding: CH: ERC Advanced Investigator Grant (Pa-CSC 233460), European Community's Seventh Framework Programme (FP7/2007-2013) under grant agreement n° 256974 (EPC-TM-NET) and n° 602783 (CAM-PaC), the Subdirección General de Evaluación y Fomento de la Investigación, Fondo de Investigación Sanitaria (PS09/02129 & PI12/02643) and the Programa Nacional de Internacionalización de la I+D, Subprogramma: FCCI 2009 (PLE2009-0105; both Ministerio de Economía y Competitividad (es), Spain), BSJr: Rámon y Cajal Merit Award from the Ministerio de Economía y Competitividad, Spain and Clinic and Laboratory Integration Program (CLIP) grant from the Cancer Research Institute, NY, NY. MC: La Caixa Predoctoral Fellowship.

Competing interests: None.

Patient consent: Obtained.

Ethics approval: Instituto de Salud Carlos III, Madrid, Spain.

Conflict of interest statement: *All authors confirm that no conflict of interests exists for the presented study*

REFERENCES

1 Paulson AS, Tran Cao HS, Tempero MA, Lowy AM. Therapeutic advances in pancreatic cancer. Gastroenterology 2013;**144**:1316-26.

2 Hermann PC, Huber SL, Herrler T, Aicher A, Ellwart JW, Guba M, *et al.* Distinct populations of cancer stem cells determine tumor growth and metastatic activity in human pancreatic cancer. Cell Stem Cell 2007;**1**:313-23.

3 Li C, Heidt DG, Dalerba P, Burant CF, Zhang L, Adsay V, *et al.* Identification of pancreatic cancer stem cells. Cancer Res 2007;**67**:1030-7.

4 Rasheed ZA, Yang J, Wang Q, Kowalski J, Freed I, Murter C, *et al.* Prognostic Significance of Tumorigenic Cells With Mesenchymal Features in Pancreatic Adenocarcinoma. J Natl Cancer Inst 2010;**102**:340-51.

5 Miranda-Lorenzo I, Dorado J, Lonardo E, Alcala S, Serrano AG, Clausell-Tormos J, *et al.* Intracellular autofluorescence: a biomarker for epithelial cancer stem cells. Nat Methods 2014;**11**:1161-9.

6 Lonardo E, Hermann PC, Mueller MT, Huber S, Balic A, Miranda-Lorenzo I, *et al.* Nodal/Activin signaling drives self-renewal and tumorigenicity of pancreatic cancer stem cells and provides a target for combined drug therapy. Cell Stem Cell 2011;**9**:433-46.

7 Mueller MT, Hermann PC, Witthauer J, Rubio-Viqueira B, Leicht SF, Huber S, *et al.* Combined targeted treatment to eliminate tumorigenic cancer stem cells in human pancreatic cancer. Gastroenterology 2009;**137**:1102-13.

8 Chu GC, Kimmelman AC, Hezel AF, DePinho RA. Stromal biology of pancreatic cancer. J Cell Biochem 2007;**101**:887-907.

9 Bachem MG, Schunemann M, Ramadani M, Siech M, Beger H, Buck A, *et al.* Pancreatic carcinoma cells induce fibrosis by stimulating proliferation and matrix synthesis of stellate cells. Gastroenterology 2005;**128**:907-21.

10 Lonardo E, Frias-Aldeguer J, Hermann PC, Heeschen C. Pancreatic stellate cells form a niche for cancer stem cells and promote their self-renewal and invasiveness. Cell Cycle 2012;**11**:1282-90.

11 Farrow B, Sugiyama Y, Chen A, Uffort E, Nealon W, Mark Evers B. Inflammatory mechanisms contributing to pancreatic cancer development. Ann Surg 2004;**239**:763-9; discussion 9-71.

12 Biswas SK, Mantovani A. Macrophage plasticity and interaction with lymphocyte subsets: cancer as a paradigm. Nat Immunol 2010;**11**:889-96.

13 Mantovani A, Sica A. Macrophages, innate immunity and cancer: balance, tolerance, and diversity. Curr Opin Immunol 2010;**22**:231-7.

14 Mantovani A, Sozzani S, Locati M, Allavena P, Sica A. Macrophage polarization: tumor-associated macrophages as a paradigm for polarized M2 mononuclear phagocytes. Trends Immunol 2002;**23**:549-55.

15 Kurahara H, Shinchi H, Mataki Y, Maemura K, Noma H, Kubo F, *et al.* Significance of M2-polarized tumor-associated macrophage in pancreatic cancer. J Surg Res 2011;**167**:e211-9.

16 Pollard JW. Tumour-educated macrophages promote tumour progression and metastasis. Nat Rev Cancer 2004;**4**:71-8.

17 Sica A, Schioppa T, Mantovani A, Allavena P. Tumour-associated macrophages are a distinct M2 polarised population promoting tumour progression: potential targets of anti-cancer therapy. Eur J Cancer 2006;**42**:717-27.

18 Coffelt SB, Waterman RS, Florez L, Honer zu Bentrup K, Zwezdaryk KJ, Tomchuck SL, *et al.* Ovarian cancers overexpress the antimicrobial protein hCAP-18 and its derivative LL-37 increases ovarian cancer cell proliferation and invasion. Int J Cancer 2008;**122**:1030-9.

19 Agerberth B, Gunne H, Odeberg J, Kogner P, Boman HG, Gudmundsson GH. FALL-39, a putative human peptide antibiotic, is cysteine-free and expressed in bone marrow and testis. Proc Natl Acad Sci U S A 1995;**92**:195-9.

20 Larrick JW, Hirata M, Balint RF, Lee J, Zhong J, Wright SC. Human CAP18: a novel antimicrobial lipopolysaccharide-binding protein. Infect Immun 1995;**63**:1291-7.

21 De Y, Chen Q, Schmidt AP, Anderson GM, Wang JM, Wooters J, *et al.* LL-37, the neutrophil granule- and epithelial cell-derived cathelicidin, utilizes formyl peptide receptor-like 1 (FPRL1) as a receptor to chemoattract human peripheral blood neutrophils, monocytes, and T cells. J Exp Med 2000;**192**:1069-74.

22 Nagaoka I, Tamura H, Hirata M. An antimicrobial cathelicidin peptide, human CAP18/LL-37, suppresses neutrophil apoptosis via the activation of formyl-peptide receptor-like 1 and P2X7. J Immunol 2006;**176**:3044-52.

23 Coffelt SB, Tomchuck SL, Zwezdaryk KJ, Danka ES, Scandurro AB. Leucine leucine-37 uses formyl peptide receptor-like 1 to activate signal transduction pathways, stimulate oncogenic gene expression, and enhance the invasiveness of ovarian cancer cells. Mol Cancer Res 2009;**7**:907-15.

24 Sierra-Filardi E, Puig-Kroger A, Blanco FJ, Nieto C, Bragado R, Palomero MI, *et al.* Activin A skews macrophage polarization by promoting a proinflammatory phenotype and inhibiting the acquisition of anti-inflammatory macrophage markers. Blood 2011;**117**:5092-101.

25 Chao MP, Alizadeh AA, Tang C, Myklebust JH, Varghese B, Gill S, *et al.* Anti-CD47 antibody synergizes with rituximab to promote phagocytosis and eradicate non-Hodgkin lymphoma. Cell 2010;**142**:699-713.

26 Verreck FA, de Boer T, Langenberg DM, van der Zanden L, Ottenhoff TH. Phenotypic and functional profiling of human proinflammatory type-1 and anti-inflammatory type-2 macrophages in response to microbial antigens and IFN-gamma- and CD40L-mediated costimulation. Journal of leukocyte biology 2006;**79**:285-93.

27 Hingorani SR, Wang L, Multani AS, Combs C, Deramaudt TB, Hruban RH, *et al.* Trp53R172H and KrasG12D cooperate to promote chromosomal instability and widely metastatic pancreatic ductal adenocarcinoma in mice. Cancer Cell 2005;**7**:469-83.

28 Nizet V, Ohtake T, Lauth X, Trowbridge J, Rudisill J, Dorschner RA, *et al.* Innate antimicrobial peptide protects the skin from invasive bacterial infection. Nature 2001;**414**:454-7.

29 Heilborn JD, Nilsson MF, Jimenez CI, Sandstedt B, Borregaard N, Tham E, *et al.* Antimicrobial protein hCAP18/LL-37 is highly expressed in breast cancer and is a putative growth factor for epithelial cells. Int J Cancer 2005;**114**:713-9.

30 Weber G, Chamorro CI, Granath F, Liljegren A, Zreika S, Saidak Z, *et al.* Human antimicrobial protein hCAP18/LL-37 promotes a metastatic phenotype in breast cancer. Breast Cancer Res 2009;**11**:R6.

31 von Haussen J, Koczulla R, Shaykhiev R, Herr C, Pinkenburg O, Reimer D, *et al.* The host defence peptide LL-37/hCAP-18 is a growth factor for lung cancer cells. Lung Cancer 2008;**59**:12-23.

32 Li D, Beisswenger C, Herr C, Schmid RM, Gallo RL, Han G, *et al.* Expression of the antimicrobial peptide cathelicidin in myeloid cells is required for lung tumor growth. Oncogene 2014;**33**:2709-16.

33 Li D, Wang X, Wu JL, Quan WQ, Ma L, Yang F, *et al.* Tumor-produced versican V1 enhances hCAP18/LL-37 expression in macrophages through activation of TLR2 and vitamin D3 signaling to promote ovarian cancer progression in vitro. PLoS One 2013;**8**:e56616.

34 Coffelt SB, Marini FC, Watson K, Zwezdaryk KJ, Dembinski JL, LaMarca HL, *et al.* The pro-inflammatory peptide LL-37 promotes ovarian tumor progression through recruitment of multipotent mesenchymal stromal cells. Proc Natl Acad Sci U S A 2009;**106**:3806-11.

35 Ren SX, Cheng AS, To KF, Tong JH, Li MS, Shen J, *et al.* Host immune defense peptide LL-37 activates caspase-independent apoptosis and suppresses colon cancer. Cancer Res 2012;**72**:6512-23.

36 Kreso A, Dick JE. Evolution of the cancer stem cell model. Cell Stem Cell 2014;**14**:275-91.

37 Hamilton TA, Zhao C, Pavicic PG, Jr., Datta S. Myeloid colony-stimulating factors as regulators of macrophage polarization. Frontiers in immunology 2014;**5**:554.

38 Heusinkveld M, de Vos van Steenwijk PJ, Goedemans R, Ramwadhdoebe TH, Gorter A, Welters MJ, *et al.* M2 macrophages induced by prostaglandin E2 and IL-6 from cervical carcinoma are switched to activated M1 macrophages by CD4+ Th1 cells. J Immunol 2011;**187**:1157-65.

39 Heusinkveld M, van der Burg SH. Identification and manipulation of tumor associated macrophages in human cancers. Journal of translational medicine 2011;**9**:216.

40 Flavell RA, Sanjabi S, Wrzesinski SH, Licona-Limon P. The polarization of immune cells in the tumour environment by TGFbeta. Nat Rev Immunol 2010;**10**:554-67.

41 Massague J. TGFbeta in Cancer. Cell 2008;**134**:215-30.

42 Iacobuzio-Donahue CA, Fu B, Yachida S, Luo M, Abe H, Henderson CM, *et al.* DPC4 gene status of the primary carcinoma correlates with patterns of failure in patients with pancreatic cancer. J Clin Oncol 2009;**27**:1806-13.

43 Tomasinsig L, Pizzirani C, Skerlavaj B, Pellegatti P, Gulinelli S, Tossi A, *et al.* The human cathelicidin LL-37 modulates the activities of the P2X7 receptor in a structure-dependent manner. J Biol Chem 2008;**283**:30471-81.

44 Gordon S. Alternative activation of macrophages. Nat Rev Immunol 2003;**3**:23-35.

45 Bonde AK, Tischler V, Kumar S, Soltermann A, Schwendener RA. Intratumoral macrophages contribute to epithelial-mesenchymal transition in solid tumors. BMC Cancer 2012;**12**:35.

46 Sainz B, Jr., Martin B, Tatari M, Heeschen C, Guerra S. ISG15 is a critical microenvironmental factor for pancreatic cancer stem cells. Cancer Res 2014;**74**:7309-20.

47 Tsai YC, Pestka S, Wang LH, Runnels LW, Wan S, Lyu YL, *et al.* Interferon-beta signaling contributes to Ras transformation. PLoS One 2011;**6**:e24291.

48 Heilborn JD, Nilsson MF, Kratz G, Weber G, Sorensen O, Borregaard N, *et al.* The cathelicidin anti-microbial peptide LL-37 is involved in re-epithelialization of human skin wounds and is lacking in chronic ulcer epithelium. J Invest Dermatol 2003;**120**:379-89.

49 Koczulla R, von Degenfeld G, Kupatt C, Krotz F, Zahler S, Gloe T, *et al.* An angiogenic role for the human peptide antibiotic LL-37/hCAP-18. J Clin Invest 2003;**111**:1665-72.

50 Rivas-Santiago B, Hernandez-Pando R, Carranza C, Juarez E, Contreras JL, Aguilar-Leon D, *et al.* Expression of cathelicidin LL-37 during Mycobacterium tuberculosis infection in human alveolar macrophages, monocytes, neutrophils, and epithelial cells. Infect Immun 2008;**76**:935-41.

51 Dai X, Sayama K, Tohyama M, Shirakata Y, Hanakawa Y, Tokumaru S, *et al.* PPARgamma mediates innate immunity by regulating the 1alpha,25-dihydroxyvitamin D3 induced hBD-3 and cathelicidin in human keratinocytes. J Dermatol Sci 2010;**60**:179-86.

52 Park K, Elias PM, Oda Y, Mackenzie D, Mauro T, Holleran WM, *et al.* Regulation of cathelicidin antimicrobial peptide expression by an endoplasmic reticulum (ER) stress signaling, vitamin D receptor-independent pathway. J Biol Chem 2011;**286**:34121-30.

53 Grosse-Steffen T, Giese T, Giese N, Longerich T, Schirmacher P, Hansch GM, *et al.* Epithelial-to-mesenchymal transition in pancreatic ductal adenocarcinoma and pancreatic tumor cell lines: the role of neutrophils and neutrophil-derived elastase. Clin Dev Immunol 2012;**2012**:720768.

54 Acharyya S, Oskarsson T, Vanharanta S, Malladi S, Kim J, Morris PG, *et al.* A CXCL1 paracrine network links cancer chemoresistance and metastasis. Cell 2012;**150**:165-78.

55 Wu W, Kim CH, Liu R, Kucia M, Marlicz W, Greco N, *et al.* The bone marrow-expressed antimicrobial cationic peptide LL-37 enhances the responsiveness of hematopoietic stem progenitor cells to an SDF-1 gradient and accelerates their engraftment after transplantation. Leukemia 2012;**26**:736-45.

56 Gombart AF, Borregaard N, Koeffler HP. Human cathelicidin antimicrobial peptide (CAMP) gene is a direct target of the vitamin D receptor and is strongly up-regulated in myeloid cells by 1,25-dihydroxyvitamin D3. FASEB J 2005;**19**:1067-77.

FIGURE LEGENDS

Figure 1: Macrophages promote PDAC tumour take and growth. (**A**) Summary of *in vivo* tumour take and growth 3 weeks post subcutaneous injection of sphere-derived CSC-enriched PDAC cells with or without human monocyte-derived unpolarized macrophages (MØ), immortalized PSCs (iPSCs) or primary PSCs (pPSCs) (n=4 mice/group). (**B**) Heatmap of top 25 genes up-regulated and down-regulated (FDR<10^{-4}, $|\log FC| > 2$) in primary human monocyte-derived macrophages co-cultured with Panc185 (1), Panc354 (2) or Panc215 (3) in a trans-well assay for 48h. (**C**) RT-qPCR analysis of hCAP18/LL-37 mRNA levels in human monocyte-derived macrophages alone or co-cultured with indicated PDAC cells for 48h. (**D**) Immunofluorescence analysis of CD16 (macrophage marker) and LL-37 in human monocyte-derived macrophage-PDAC cell co-cultures. White dashed line marks the perimeter of a PDAC colony. Scale bar = 100µm. (**E**) RT-qPCR analysis of Oct3/4 and Nanog mRNA levels in Panc215 and Panc185 cultures following 48h co-cultivation with primary human monocyte-derived macrophages in a trans-well assay.

Figure 2: LL-37 expression is restricted to the tumour stroma and correlates with advanced neoplastic lesions. (**A**) RT-qPCR analysis of hCAP18/LL-37 mRNA levels in a panel of surgically resected human primary PDAC tumours (n=30 tumours) and cultures. WB analysis of hCAP18/LL-37 protein expression in a subgroup of samples (inset). (**B**) hCAP18/LL-37 expression profile in a TMA panel containing normal, PanIN (I-III), PDAC, metastases and pancreatitis cores. (**C**) Representative micrographs of hCAP18/LL-37-stained TMA cores. (**D**) Serial sections of a PDAC TMA core stained for hCAP18/LL-37, the macrophage markers CD16, and the PSC marker αSMA. (**E**) Immunohistological analysis of CRAMP (murine ortholog of LL-37) and YM1 (macrophage marker) expression in 26-week old KPC mouse pancreas and liver. Scale bars = 200 and 50µm (insets). nPanc = normal pancreas.

Figure 3: CRAMP affects PDAC tumour growth *in vivo*. (**A**) IHC analysis of CRAMP expression in representative FFPE sections from pancreata of 22-23-week old KPC mice transplanted with bone marrow from wild-type control C57Bl/6 mice or $CRAMP^{-/-}$ mice (n=4 mice/group). (**B**) Quantification of

tissue area in mouse pancreata from 22-23-week old KPC mice transplanted with bone marrow from wild-type control C57Bl/6 mice (n=4 mice) or CRAMP$^{-/-}$ mice (n=4 mice/group), categorized as normal acinar tissue, severely altered tissue (ADM and inflammation) or tumour tissue (PanINs I-III and PDAC) (**Fig. S5B**). Representative images of tumour tissue (**right**). (**C** and **D**) Wild-type and CRAMP$^{-/-}$ mice were subcutaneously injected with the indicated number of primary murine PDAC cells (ie, CHX-BC-RFP-Luc cells) in Matrigel^{TM} (n=8 injections/group). Tumour take was determined 5 weeks post-injection (**left**) by BLI assessment (**C**). Representative BLI pictures of mice 5 weeks post injection with indicated numbers of murine PDAC cells (**left**). Summary of *in vivo* tumour take and growth (**right**). CSC frequencies determined using the extreme limiting dilution analysis algorithm (http://bioinf.wehi.edu.au/software/elda/index.htmL) (**right**, 95% CI). (**D**) Tumours from mice injected with 10^5 murine PDAC cells were excised and CD133 content within the RFP+ population was determined. Quantification of the percent of cells expressing CD133 is graphed (**top**) and representative cytometry plots are shown (**bottom**). (**E**) Summary of *in vivo* tumour take and growth of subcutaneously-injected 5×10^5 sphere-derived CSC-enriched murine PDAC cells with or without murine monocyte-derived unpolarized macrophages (MØ) isolated from wild-type (wt) CRAMP$^{+/+}$ mice or CRAMP$^{-/-}$ mice (n=8 mice/group). n.s. = not significant.

Figure 4: **LL-37 expands the CSC pool.** (**A** and **B**) Primary sphere-derived PDAC cultures were treated with rLL-37 and the percentage of (**A**) CD133+ cells and (**B**) autofluorescent cells was measured by flow cytometry. (**C** and **D**) Effects of rLL-37 on CSC (**C**) colony formation and (**D**) serial sphere formation. (**E**) RT-qPCR analysis of pluripotency-associated genes in sphere-derived PDAC cells after stimulation with rLL-37. (**F**) Percentage of CD133+ cells in control vs. Gemcitabine (GEM)-treated (0.1µg/mL) or Gemcitabine and rLL-37-treated (5µg/mL) primary PDAC cells (top), as determined by flow cytometric analysis (bottom).

Figure 5: LL-37 enhances functional CSC properties. (**A** and **B**) Mice were subcutaneously injected with the indicated number of scrambled or rLL-37 peptide (10µg/mL) pre-treated CSCs resuspended in Matrigel^{TM} (n=4 mice/dilution/group). (**A**) Tumour take was determined 10 weeks post-injection (left).

Images of resected tumours and CSC frequencies determined using the extreme limiting dilution analysis algorithm (http://bioinf.wehi.edu.au/software/elda/index.htmL) (**right**, 95% CI). (**B**) Summary of *in vivo* tumour take and growth. (**C**) Primary PDAC cells were sorted for the CSC marker CD133, treated with rLL-37 or a scrambled peptide control, cultured as spheres in anchorage independent conditions and sphere numbers determined 7 days later (n.s. = not significant). (**D**) Proliferation, as detected by BrdU staining, in CD133+ and CD133– PDAC cells after stimulation with rLL-37.

Figure 6: LL-37 promotes EMT and CSC invasiveness. (**A**) Flow cytometry analysis of CXCR4 cell surface expression in 2 primary PDAC cultures treated with rLL-37. (**B**) RT-qPCR analysis of EMT genes in sphere-derived PDAC cells after stimulation with rLL-37. (**C**) Western blot analysis of E-cadherin, vimentin and GAPDH in PDAC cells after stimulation with rLL-37 (**left**) and densitometric analysis of blots (**right**). RDU = relative density units. (**D**) Scratch wound assay of PDAC cells after stimulation with rLL-37. Representative micrographs (left) and quantification of wound size 12h after wound induction (**right**). (**E**) Representative images of invaded cells (**left**) and quantification of invaded rLL-37-treated PDAC cells through Matrigel™ following stimulation with 20% FBS (+Ctl), media alone (-Ctl) or increasing concentration of SDF-1 (**right**). (**F**) PDAC cells dissemination *in vivo*, assessed by noninvasive bioluminescence imaging (BLI) at 10 weeks after intrasplenic injection of luciferase expressing rLL-37-treated (10µg/mL) PDAC cells in NOD scid IL2 receptor γ chain knockout (NSG) mice (**tops**) and BLI assessment of PDAC cell dissemination to the liver (**bottoms**) (n=5 mice/group). (**G**) Dissemination of PDAC-luciferase cells to the liver was further verified by measuring luciferase activity in explanted and homogenized tissues, expressed as relative light units (RLUs)/mg of total protein.

Figure 7: Macrophages express hCAP-18/LL-37 in response to CSC-secreted TGF-β1, Nodal and ActivinA. (**A**) RT-qPCR analysis of hCAP18/LL-37 mRNA levels in human monocyte-derived macrophages cultured with control media or CSC conditioned-media (CM). (**B**) Western blot analysis of hCAP18/LL-37 and GAPDH in human monocyte-derived macrophages cultured with control media or CSC CM (left) and corresponding densitometric analysis (**right**). **(C)** Representative micrographs of

primary monocyte-derived macrophages cultured with control media or CSC CM. (**D**) RT-qPCR analysis of hCAP18/LL-37, OSM and VEGF mRNA expression levels in human monocyte-derived macrophages cultured with control media or with CSC CM from 3 primary PDAC cultures. (**E-G**) Primary human monocyte-derived macrophages were cultured with control media or with CSC CM, TGF-β□ (1ng/mL), Nodal (300ng/mL) and ActivinA (100ng/mL) or a combination of all three. (**E**) RT-qPCR analysis of hCAP18/LL-37 mRNA levels, (**F**) western blot analysis of hCAP18/LL-37, pSmad2, total Smad2 and GAPDH, (**G**) RT-qPCR analysis of OSM and VEGF mRNA levels. (**H**) RT-qPCR analysis of hCAP18/LL-37, OSM and VEGF mRNA levels in primary human monocyte-derived macrophages pre-treated for 1 h with a diluent control (Ctl), SB431542 (20μM) or SB505124 (20μM) and subsequently cultured for 48h with control media, CSC CM, TGF-β□ (1ng/mL), or Nodal (300ng/mL) and Activin (100ng/mL). n.s. = not significant.

Figure 8: Targeting LL-37 receptors inhibit CSC phenotypes. (**A**) Diagram of the cross-talk between macrophages and CSCs, receptors and secreted factors involved, and specific inhibitors of these pathways. (**B**) RT-qPCR analysis of FPR2 and P2X7R mRNA levels in 3 primary PDAC cultures. (**C**) Flow cytometry analysis of P2X7R cell surface expression in 2 primary PDAC lines cultured as adherent or sphere cultures and treated with rLL-37. Percentage of CD133-positive cells within the P2X7R-positive subpopulation is shown in the right panels. (**D** and **E**) LL-37-treated sphere-derived PDAC cells were pre-treated with diluent control or WR-W4, KN-62 or a combination of both and (**D**) colony formation on Matrigel™, (**E**) invasion through Matrigel™ following stimulation with SDF-1 (+Ctrl = 20% FBS; –Ctrl = media alone) or (F) the percentage of CD133-positive cells measured by flow cytometry was determined.

Figure 9: Targeting LL-37 receptors inhibit PDAC development *in vivo*. (**A**) Experimental setup for *in vivo* short-term and long-term treatment. (**B**) Analysis of serum CTCs (RFP+). Representative flow cytometry plots are shown (**left**) and quantification of the frequency of circulating tumour cells/lineage negative cells following 5 weeks of treatment are shown (**right**) (n=4 mice/group). (**C**) Representative images of mouse pancreata from control (n=4 mice) vs. treated (n=4 mice) *KPC* mice after 5 weeks of

treatment (**left**). Quantitative analysis of PanIN/PDAC frequency and grading (**right**). n.s. = not significant. (**D**) Analysis of serum CTCs (EPCAM+). Representative flow cytometry plots are shown (l**eft**) and quantification of the frequency of circulating tumour cells/lineage negative cells following 16 weeks of treatment are shown (**right**) (n=4 mice/group). (**E**) Representative images of mouse pancreata from control (n=4 mice) vs. treated (n=4 mice) *KPC* mice after 16 weeks of treatment (**left**). Quantitative analysis of PanIN/PDAC frequency and grading (**right**).

Figure 1 – Macrophages promote PDAC tumourigenesis and produce hCAP-18/LL-37

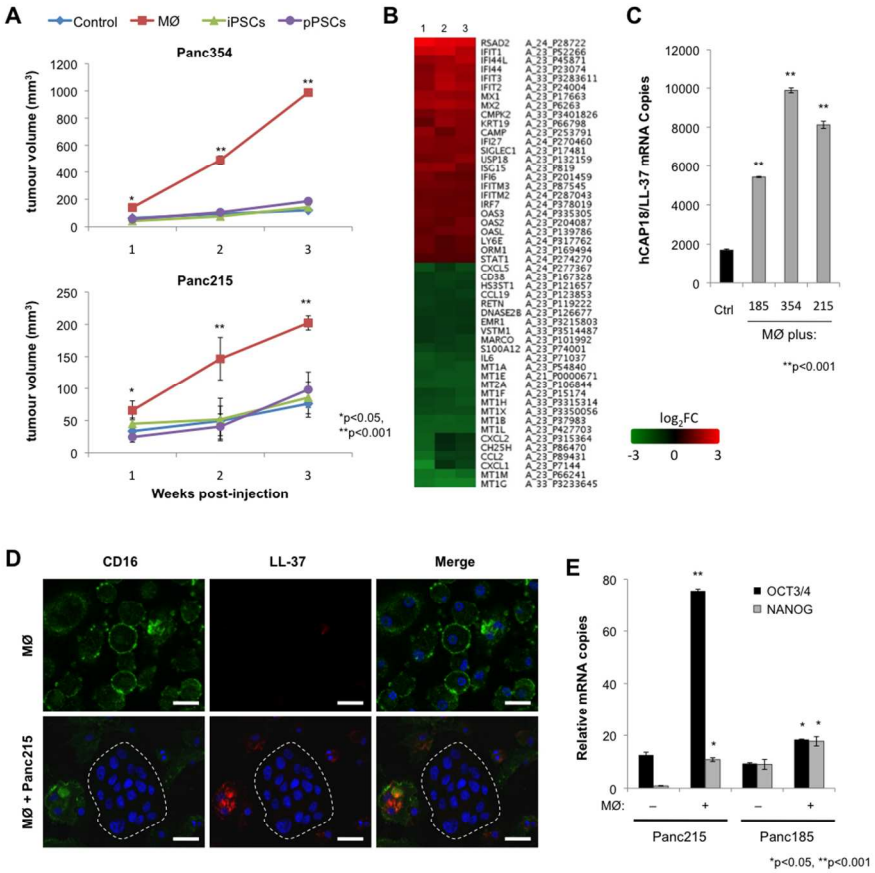

Figure 1: Macrophages promote PDAC tumour take and growth. (A) Summary of in vivo tumour take and growth 3 weeks post subcutaneous injection of sphere-derived CSC-enriched PDAC cells with or without human monocyte-derived unpolarized macrophages (MØ), immortalized PSCs (iPSCs) or primary PSCs (pPSCs) (n=4 mice/group). (B) Heatmap of top 25 genes up-regulated and down-regulated (FDR<10-4, |logFC| > 2) in primary human monocyte-derived macrophages co-cultured with Panc185 (1), Panc354 (2) or Panc215 (3) in a trans-well assay for 48h. (C) RT-qPCR analysis of hCAP18/LL-37 mRNA levels in human monocyte-derived macrophages alone or co-cultured with indicated PDAC cells for 48h. (D) Immunofluorescence analysis of CD16 (macrophage marker) and LL-37 in human monocyte-derived macrophage-PDAC cell co-cultures. White dashed line marks the perimeter of a PDAC colony. Scale bar = 100µm. (E) RT-qPCR analysis of Oct3/4 and Nanog mRNA levels in Panc215 and Panc185 cultures following 48h co-cultivation with primary human monocyte-derived macrophages in a trans-well assay.
388x513mm (72 x 72 DPI)

Figure 2 – LL-37 expression is restricted to the tumour stroma and correlates with advanced neoplastic lesions

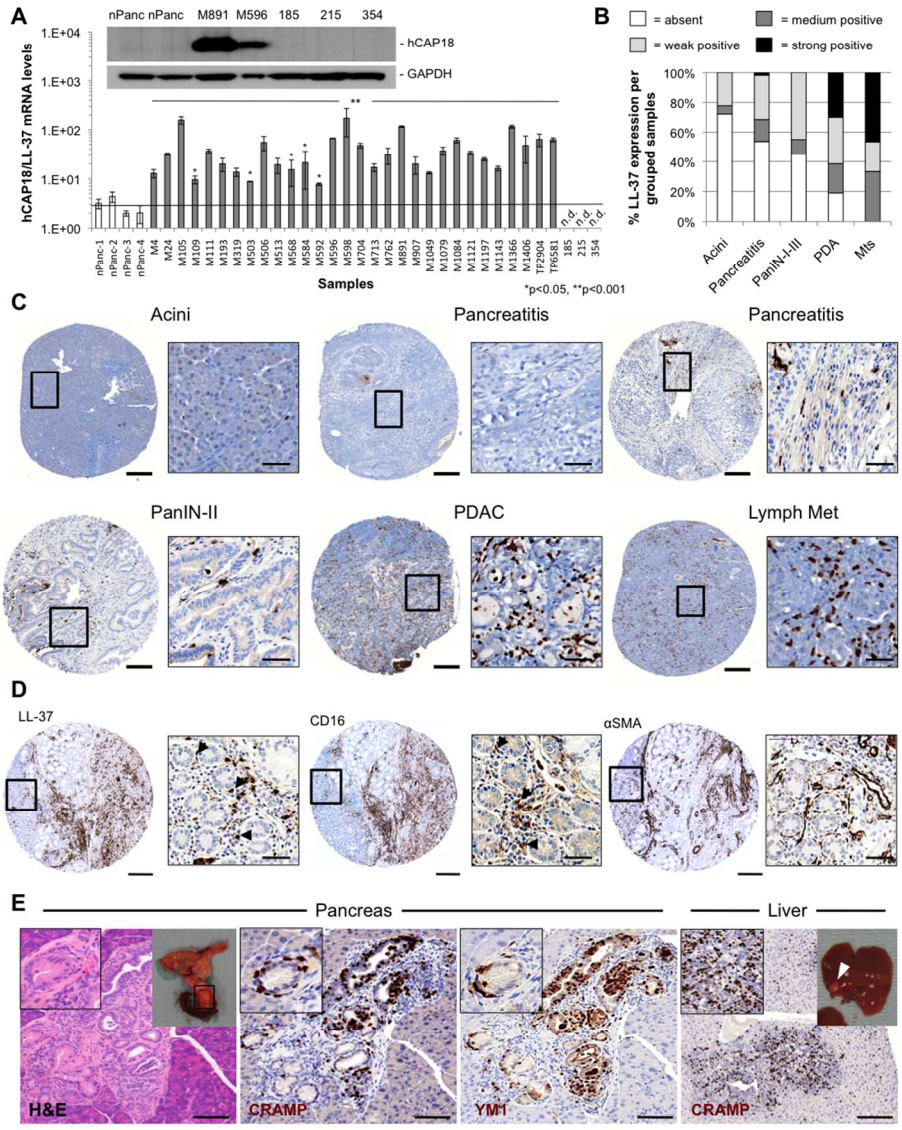

Figure 2: LL-37 expression is restricted to the tumour stroma and correlates with advanced neoplastic lesions. (A) RT-qPCR analysis of hCAP18/LL-37 mRNA levels in a panel of surgically resected human primary PDAC tumours (n=30 tumours) and cultures. WB analysis of hCAP18/LL-37 protein expression in a subgroup of samples (inset). (B) hCAP18/LL-37 expression profile in a TMA panel containing normal, PanIN (I-III), PDAC, metastases and pancreatitis cores. (C) Representative micrographs of hCAP18/LL-37-stained TMA cores. (D) Serial sections of a PDAC TMA core stained for hCAP18/LL-37, the macrophage markers CD16, and the PSC marker αSMA. (E) Immunohistological analysis of CRAMP (murine ortholog of LL-37) and YM1 (macrophage marker) expression in 26-week old KPC mouse pancreas and liver. Scale bars = 200 and 50μm (insets). nPanc = normal pancreas.
388x513mm (72 x 72 DPI)

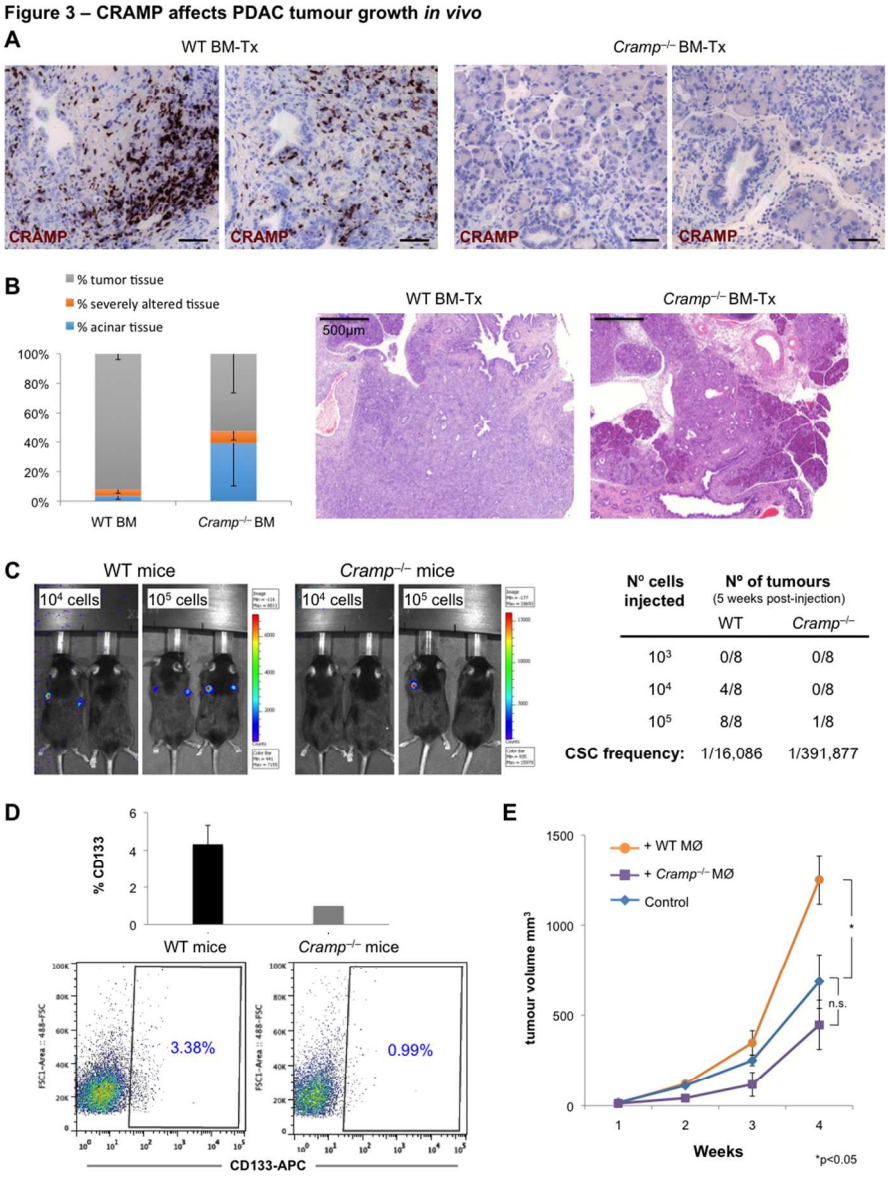

Figure 3: CRAMP affects PDAC tumour growth in vivo. (A) IHC analysis of CRAMP expression in representative FFPE sections from pancreata of 22-23-week old KPC mice transplanted with bone marrow from wild-type control C57Bl/6 mice or CRAMP–/– mice (n=4 mice/group). (B) Quantification of tissue area in mouse pancreata from 22-23-week old KPC mice transplanted with bone marrow from wild-type control C57Bl/6 mice (n=4 mice) or CRAMP–/– mice (n=4 mice/group), categorized as normal acinar tissue, severely altered tissue (ADM and inflammation) or tumour tissue (PanINs I-III and PDAC) (Fig. S5B). Representative images of tumour tissue (right). (C and D) Wild-type and CRAMP–/– mice were subcutaneously injected with the indicated number of primary murine PDAC cells (ie, CHX-BC-RFP-Luc cells) in Matrigel™ (n=8 injections/group). Tumour take was determined 5 weeks post-injection (left) by BLI assessment (C). Representative BLI pictures of mice 5 weeks post injection with indicated numbers of murine PDAC cells (left). Summary of in vivo tumour take and growth (right). CSC frequencies determined using the extreme limiting dilution analysis algorithm (http://bioinf.wehi.edu.au/software/elda/index.html) (right, 95% CI). (D) Tumours from mice injected with 105 murine PDAC cells were excised and CD133

content within the RFP+ population was determined. Quantification of the percent of cells expressing CD133 is graphed (top) and representative cytometry plots are shown (bottom). (E) Summary of in vivo tumour take and growth of subcutaneously-injected 5×105 sphere-derived CSC-enriched murine PDAC cells with or without murine monocyte-derived unpolarized macrophages (MØ) isolated from wild-type (wt) CRAMP+/+ mice or CRAMP−/− mice (n=8 mice/group). n.s. = not significant.
388x513mm (72 x 72 DPI)

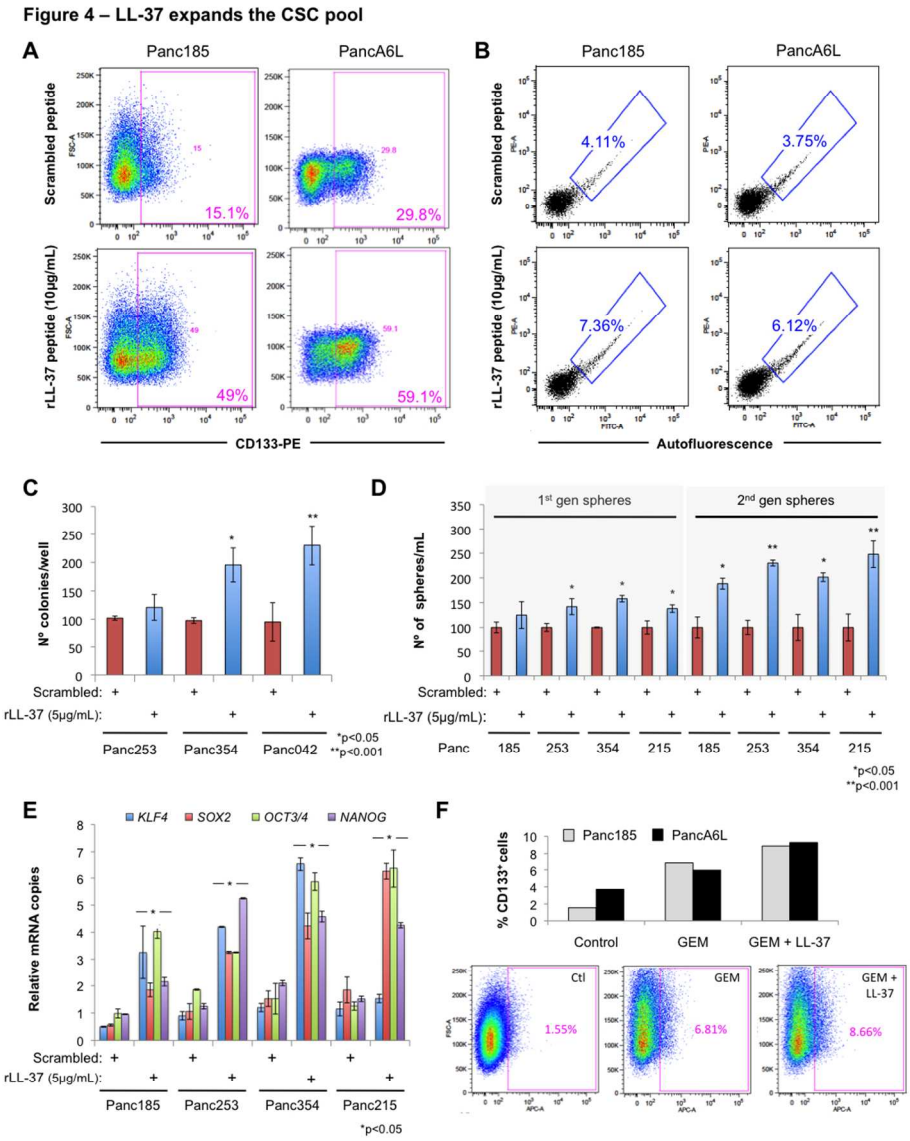

Figure 4: LL-37 expands the CSC pool. (A and B) Primary sphere-derived PDAC cultures were treated with rLL-37 and the percentage of (A) CD133+ cells and (B) autofluorescent cells was measured by flow cytometry. (C and D) Effects of rLL-37 on CSC (C) colony formation and (D) serial sphere formation. (E) RT-qPCR analysis of pluripotency-associated genes in sphere-derived PDAC cells after stimulation with rLL-37. (F) Percentage of CD133+ cells in control vs. Gemcitabine (GEM)-treated (0.1µg/mL) or Gemcitabine and rLL-37-treated (5µg/mL) primary PDAC cells (top), as determined by flow cytometric analysis (bottom). 388x513mm (72 x 72 DPI)

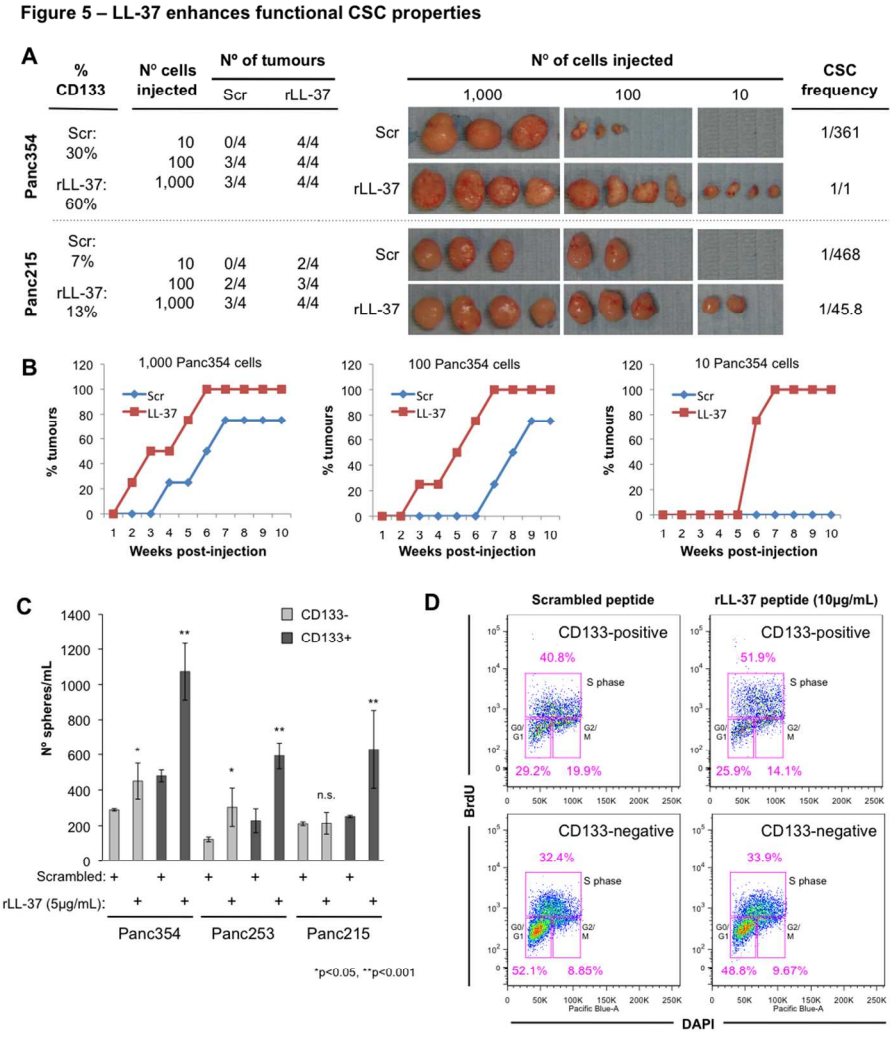

Figure 5: LL-37 enhances functional CSC properties. (A and B) Mice were subcutaneously injected with the indicated number of scrambled or rLL-37 peptide (10μg/ml) pre-treated CSCs resuspended in Matrigel™ (n=4 mice/dilution/group). (A) Tumour take was determined 10 weeks post-injection (left). Images of resected tumours and CSC frequencies determined using the extreme limiting dilution analysis algorithm (http://bioinf.wehi.edu.au/software/elda/index.html) (right, 95% CI). (B) Summary of in vivo tumour take and growth. (C) Primary PDAC cells were sorted for the CSC marker CD133, treated with rLL-37 or a scrambled peptide control, cultured as spheres in anchorage independent conditions and sphere numbers determined 7 days later (n.s. = not significant). (D) Proliferation, as detected by BrdU staining, in CD133+ and CD133– PDAC cells after stimulation with rLL-37.
388x513mm (72 x 72 DPI)

Figure 6 – LL-37 promotes EMT and CSC invasiveness

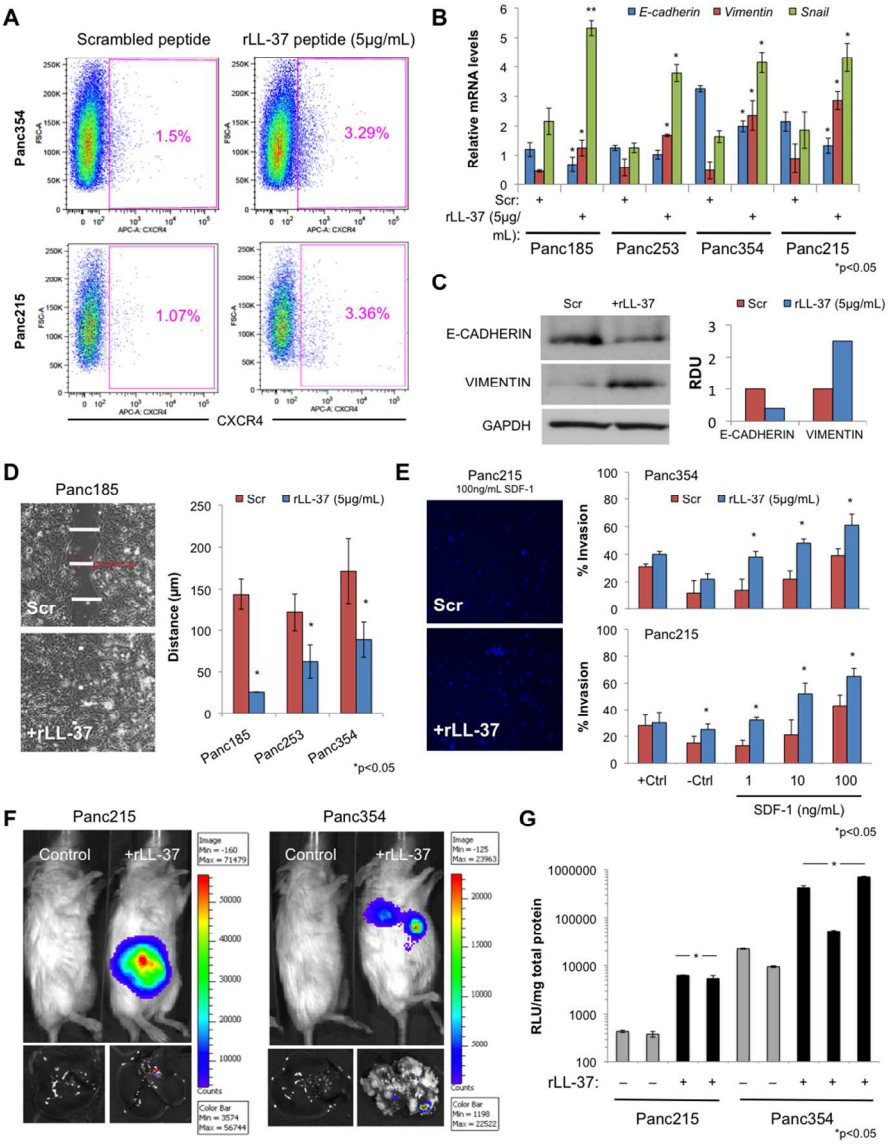

Figure 6: LL-37 promotes EMT and CSC invasiveness. (A) Flow cytometry analysis of CXCR4 cell surface expression in 2 primary PDAC cultures treated with rLL-37. (B) RT-qPCR analysis of EMT genes in sphere-derived PDAC cells after stimulation with rLL-37. (C) Western blot analysis of E-cadherin, vimentin and GAPDH in PDAC cells after stimulation with rLL-37 (left) and densitometric analysis of blots (right). RDU = relative density units. (D) Scratch wound assay of PDAC cells after stimulation with rLL-37. Representative micrographs (left) and quantification of wound size 12h after wound induction (right). (E) Representative images of invaded cells (left) and quantification of invaded rLL-37-treated PDAC cells through MatrigelTM following stimulation with 20% FBS (+Ctl), media alone (-Ctl) or increasing concentration of SDF-1 (right). (F) PDAC cells dissemination in vivo, assessed by noninvasive bioluminescence imaging (BLI) at 10 weeks after intrasplenic injection of luciferase expressing rLL-37-treated (10µg/ml) PDAC cells in NOD scid IL2 receptor γ chain knockout (NSG) mice (tops) and BLI assessment of PDAC cell dissemination to the liver (bottoms) (n=5 mice/group). (G) Dissemination of PDAC-luciferase cells to the liver was further verified by measuring luciferase activity in explanted and homogenized tissues, expressed as relative light units

(RLUs)/mg of total protein.
388x513mm (72 x 72 DPI)

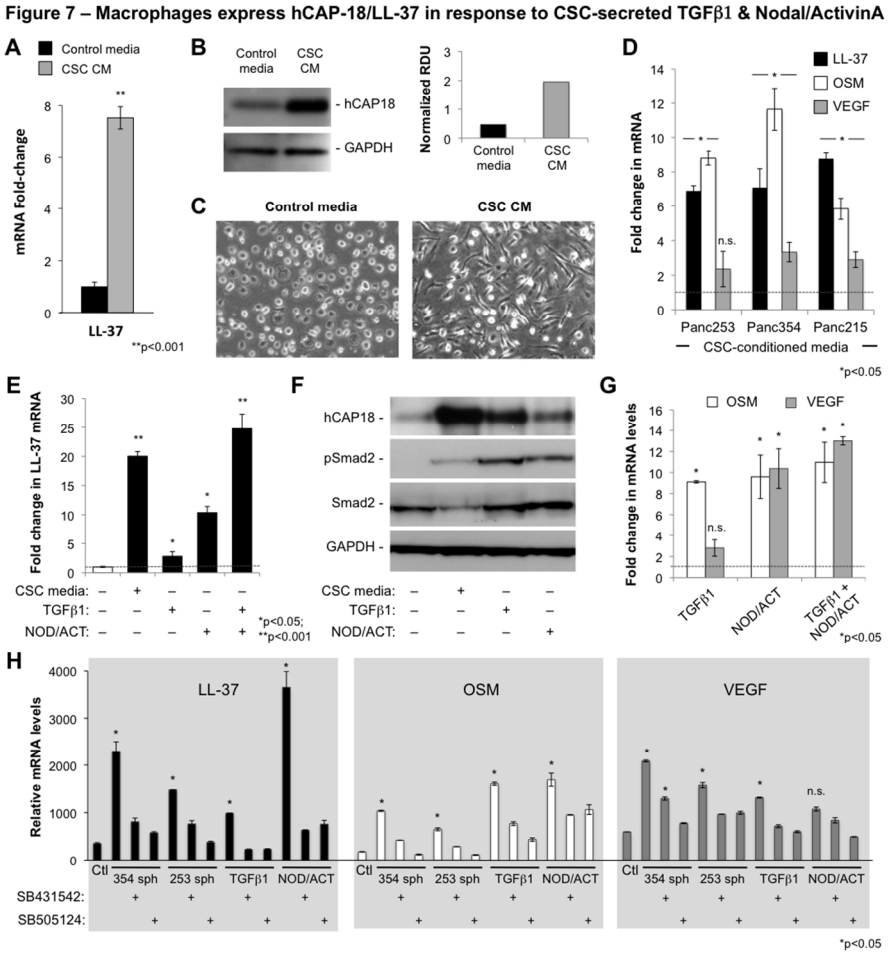

Figure 7: Macrophages express hCAP-18/LL-37 in response to CSC-secreted TGF-β1, Nodal and ActivinA. (A) RT-qPCR analysis of hCAP18/LL-37 mRNA levels in human monocyte-derived macrophages cultured with control media or CSC conditioned-media (CM). (B) Western blot analysis of hCAP18/LL-37 and GAPDH in human monocyte-derived macrophages cultured with control media or CSC CM (left) and corresponding densitometric analysis (right). (C) Representative micrographs of primary monocyte-derived macrophages cultured with control media or CSC CM. (D) RT-qPCR analysis of hCAP18/LL-37, OSM and VEGF mRNA expression levels in human monocyte-derived macrophages cultured with control media or with CSC CM from 3 primary PDAC cultures. (E-G) Primary human monocyte-derived macrophages were cultured with control media or with CSC CM, TGF-β1 (1ng/mL), Nodal (300ng/mL) and ActivinA (100ng/mL) or a combination of all three. (E) RT-qPCR analysis of hCAP18/LL-37 mRNA levels, (F) western blot analysis of hCAP18/LL-37, pSmad2, total Smad2 and GAPDH, (G) RT-qPCR analysis of OSM and VEGF mRNA levels. (H) RT-qPCR analysis of hCAP18/LL-37, OSM and VEGF mRNA levels in primary human monocyte-derived macrophages pre-treated for 1 h with a diluent control (Ctl), SB431542 (20μM) or SB505124 (20μM) and

subsequently cultured for 48h with control media, CSC CM, TGF-β1 (1ng/mL), or Nodal (300ng/mL) and Activin (100ng/mL). n.s. = not significant.
388x513mm (72 x 72 DPI)

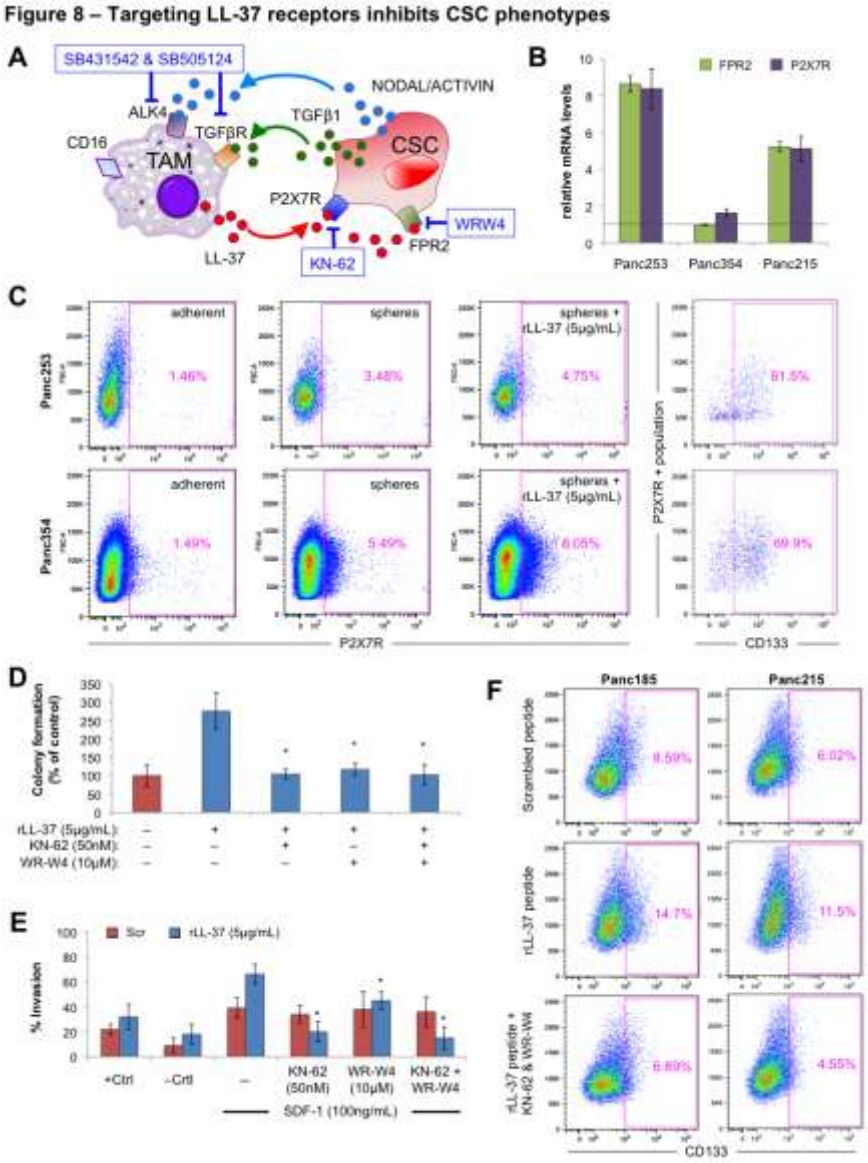

Figure 8: Targeting LL-37 receptors inhibit CSC phenotypes. (A) Diagram of the cross-talk between macrophages and CSCs, receptors and secreted factors involved, and specific inhibitors of these pathways. (B) RT-qPCR analysis of FPR2 and P2X7R mRNA levels in 3 primary PDAC cultures. (C) Flow cytometry analysis of P2X7R cell surface expression in 2 primary PDAC lines cultured as adherent or sphere cultures and treated with rLL-37. Percentage of CD133-positive cells within the P2X7R-positive subpopulation is shown in the right panels. (D and E) LL-37-treated sphere-derived PDAC cells were pre-treated with diluent control or WR-W4, KN-62 or a combination of both and (D) colony formation on Matrigel™, (E) invasion through MatrigelTM following stimulation with SDF-1 (+Ctrl = 20% FBS; –Ctrl = media alone) or (F) the percentage of CD133-positive cells measured by flow cytometry was determined.
388x513mm (72 x 72 DPI)

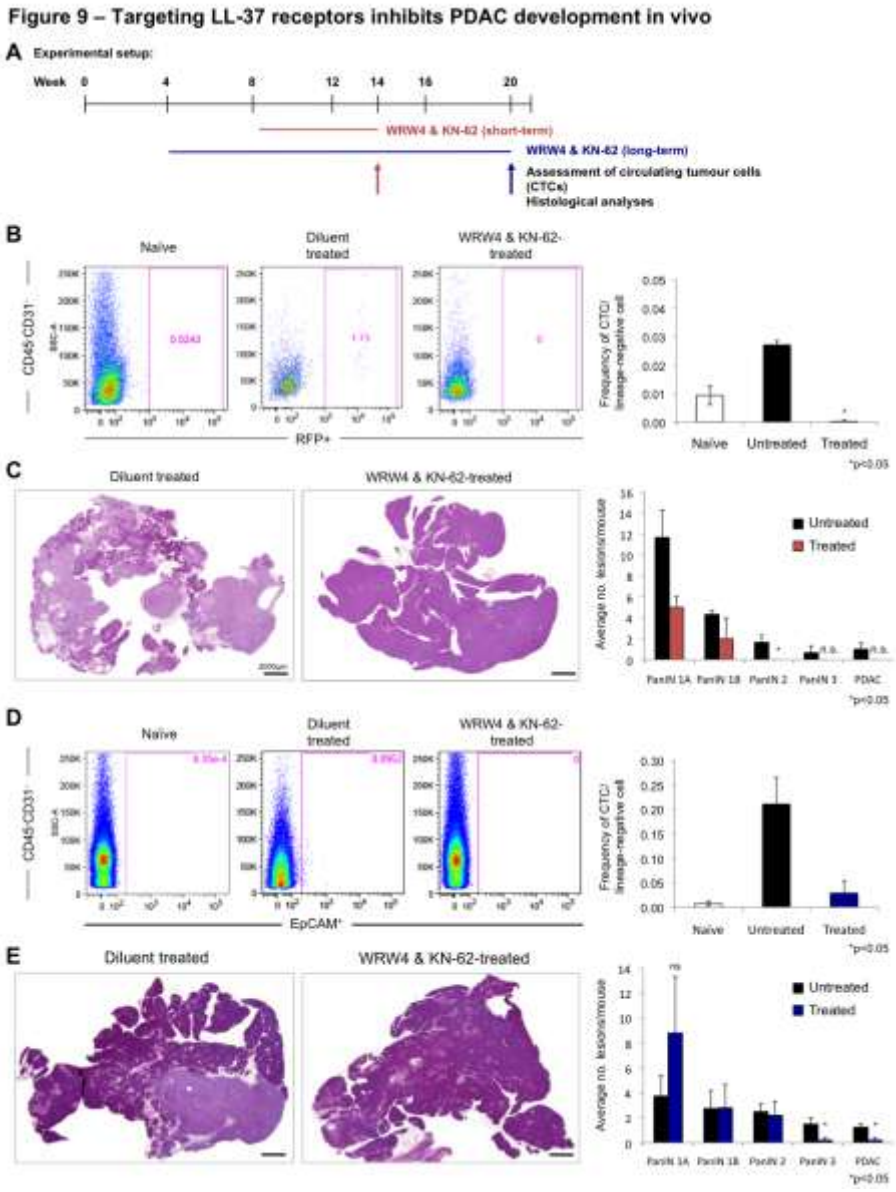

Figure 9: Targeting LL-37 receptors inhibit PDAC development in vivo. (A) Experimental setup for in vivo short-term and long-term treatment. (B) Analysis of serum CTCs (RFP+). Representative flow cytometry plots are shown (left) and quantification of the frequency of circulating tumour cells/lineage negative cells following 5 weeks of treatment are shown (right) (n=4 mice/group). (C) Representative images of mouse pancreata from control (n=4 mice) vs. treated (n=4 mice) KPC mice after 5 weeks of treatment (left). Quantitative analysis of PanIN/PDAC frequency and grading (right). n.s. = not significant. (D) Analysis of serum CTCs (EPCAM+). Representative flow cytometry plots are shown (left) and quantification of the frequency of circulating tumour cells/lineage negative cells following 16 weeks of treatment are shown (right) (n=4 mice/group). (E) Representative images of mouse pancreata from control (n=4 mice) vs. treated (n=4 mice) KPC mice after 16 weeks of treatment (left). Quantitative analysis of PanIN/PDAC frequency and grading (right).
388x513mm (72 x 72 DPI)